Single-Electrode-Based Sliding Triboelectric Nanogenerator for Self-Powered Displacement Vector Sensor System

Ya Yang,[†] Hulin Zhang,[†] Jun Chen,[†] Qingshen Jing,[†] Yu Sheng Zhou,[†] Xiaonan Wen,[†] and Zhong Lin Wang[†,‡,*]

[†]School of Materials Science and Engineering, Georgia Institute of Technology, Atlanta, Georgia 30332-0245, United States and [‡]Beijing Institute of Nanoenergy and Nanosystems, Chinese Academy of Sciences, Beijing, China

ABSTRACT We report a single-electrode-based sliding-mode triboelectric nanogenerator (TENG) that not only can harvest mechanical energy but also is a self-powered displacement vector sensor system for touching pad technology. By utilizing the relative sliding between an electrodeless polytetrafluoroethylene (PTFE) patch with surface-etched nanoparticles and an Al electrode that is grounded, the fabricated TENG can produce an open-circuit voltage up to 1100 V, a short-circuit current density of 6 mA/m^2, and a maximum power density of 350 mW/m^2 on a load of 100 MΩ, which can be used to instantaneously drive 100 green-light-emitting diodes (LEDs). The working mechanism of the TENG is based on the charge transfer between the Al electrode and the ground by modulating the relative sliding distance between the tribo-charged PTFE patch and the Al plate. Grating of linear rows on the Al electrode enables the detection of the sliding speed of the PTFE patch along one direction. Moreover, we demonstrated that 16 Al electrode channels arranged along four directions were used to monitor the displacement (the direction and the location) of the PTFE patch at the center, where the output voltage signals in the 16 channels were recorded in real-time to form a mapping figure. The advantage of this design is that it only requires the bottom Al electrode to be grounded and the top PTFE patch needs no electrical contact, which is beneficial for energy harvesting in automobile rotation mode and touch pad applications.

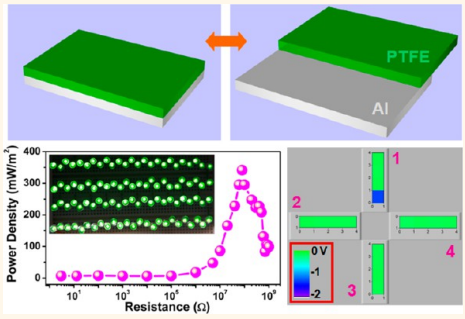

KEYWORDS: triboelectric nanogenerator · self-powered · polytetrafluoroethylene · displacement sensor · power density · touch pad

Harvesting mechanical energy from ambient environment has attracted increasing attention in the past decade not only for meeting the rapid-growing energy consumptions but also for realizing the self-powered sensor systems and achieving some electrochemical applications.[1−3] Various effects for scavenging mechanical energy have been developed such as electromagnetics,[4,5] piezoelectrics,[6,7] and electrostatics.[8,9] Based on the coupling between triboelectrification and electrostatic induction, the recently invented triboelectric nanogenerator (TENG) has been utilized to harvest random mechanical energy.[10−12] However, the previously demonstrated TENGs are all based on the vertical/horizontal separation of two tribo-charged thin film materials coated with metal electrodes for electric output. It is critical to develop new approaches to fabricate the TENGs without the need of depositing the metal electrodes on the triboelectric film materials so that we can build an electrodeless TENG for "wireless" application, which can effectively reduce the fabrication cost of the devices and achieve some new applications, such as energy harvesting from a rotating tire or touch pad sensor.

The purpose of developing self-powered nanotechnology is to drive the sensors by scavenging energy from its working environment instead of the external power sources or the conventional batteries.[13,14] TENGs have been used as self-powered sensors for sensing mercury ions, catechin, and change of magnetic field.[15−17] Usually, displacement vector sensors are capable of high-resolution measurement of the movement position and direction of the target object,[18] which have a wide variety of

* Address correspondence to zlwang@gatech.edu.

Received for review June 14, 2013 and accepted July 19, 2013.

Published online July 24, 2013
10.1021/nn403021m

applications including assembly of precision equipment, machine tool metrology, safety monitoring, and human−machine interfaces.[19] The reported displacement sensors are usually based on the optical, thermal, or magnetic sensing mechanism, where an external power source is mandatory for driving these sensors.[20−22]

In this paper, we present the single-electrode-based sliding TENG that is based on the periodic overlapping and separation between a polytetrafluoroethylene (PTFE) patch and an Al electrode by the relatively sliding motion. Due to the coupling between the triboelectric effect and electrostatic effect, the periodic change in the contact area between two surfaces can result in the charge transfer between the Al electrode and the ground, thus driving the flow of electrons in an external load. The working principle has been also elaborated by using the finite-element simulation. The maximum power density of the TENG is about 350 mW/m^2 at a load of 100 MΩ. The TENG can be used to drive 100 green-light-emitting diodes (LEDs) instantaneously. The sliding speed of the PTFE patch on the Al electrode along one direction can be detected by grating of linear rows on the Al electrode. Moreover, we demonstrated the application of TENGs as a self-powered displacement vector sensor system for detecting the motion of an object without the use of an external power source. The output voltage signals from 16 Al electrode channels were recorded in real time as a mapping figure. The motion direction and location of the object can be obtained by the analysis of the measured mapping figures. This work is an important progress toward the practical applications of the TENG-based mechanical harvesting techniques and the self-powered sensor systems.

RESULTS AND DISCUSSION

Figure 1a illustrates a schematic diagram of the fabricated TENG, which consists of a triboelectric PTFE patch and an Al plate, where the Al plays dual roles of a triboelectric surface and an electrode. The PTFE patch and the Al plate are kept in parallel to each other, where the inner surfaces are in intimate contact. The two plates slide against each other, with the contact area changing periodically by the mechanical motion along the short-edge of the plates. Usually, the output performance of the TENG can be enhanced by increasing the surface roughness and the effective surface area of the triboelectric materials to induce a larger triboelectric charge density. To increase the triboelectric charge density on the surface of the PTFE, it can be dry-etched using inductively coupled plasma (ICP) to create the nanoparticle structures. Figure 1b shows a scanning electron microscopy (SEM) image of the etched PTFE surface, which is uniformly covered with the nanoparticle structures with an average diameter of about 200 nm. The etched surface of PTFE was further characterized by the atomic force microscope (AFM), showing the same nanoparticle structures on the surface, as illustrated in Figure 1c. Figure 1d shows the output performance of the single-electrode-based TENG, where the V_{oc} can reach 1100 V with a peak J_{sc} of 6 mA/m^2. To confirm that the obtained output signals in Figure 1d were generated by the TENG, the produced energy was used to directly drive 100 green LEDs under the fast sliding motion of the PTFE on the Al plate, as shown in Figure 1e. In order to clearly demonstrate the AC output, these LEDs were divided into two groups in series (Supporting Information Figure S1), which were connected to the TENG. Under a low sliding frequency, the two LED groups were alternately lighted up, as shown in the movie file 1 (see the Supporting Information). The lifetime of the fabricated TENG can be up to several tens of years by increasing the thickness of PTFE film.

The mechanism of the single-electrode-based sliding TENG is schematically depicted in Figure 2a. In the original position, the surfaces of PTFE and Al fully overlap and intimately contact each other. According to the triboelectric series,[23] the contact between the PTFE and Al will result in electrons that are injected from Al to PTFE since PTFE is much more triboelectrically negative than Al. The produced negative triboelectric charges can be preserved on the PTFE surface for a long time due to the nature of the insulator.[24] Once the top PTFE with the negatively charged surface starts to slide outward, it will result in the decrease of the induced positive charges on the Al, thus the electrons flow from ground to Al, producing a positive current signal. When the top PTFE fully slides out of the bottom Al, the two triboelectric-charged surfaces are entirely separated, and then an equilibrium state can be created with no output voltage/current. When the top PTFE plate is reverted to slide backward, the induced positive charges on the Al increase, driving the electrons to flow from Al to the ground to produce a negative current signal. Once the two plates completely reach the overlapping position, the charged surfaces fully contact again and there will be no change of the induced charges on the Al, thus no output current can be observed. This is a full cycle of the single-electrode-based sliding TENG working process.

The electric potential distribution in the TENG and the charge transfer between the Al and the ground can be verified through numerical simulation using COMSOL. The proposed model is based on a PTFE patch and an Al plate with the same dimensions (5 cm × 8 cm × 0.1 cm), as shown in the inset of Figure 2b. The triboelectric charge density on the PTFE was assumed to be −10 μC/m^2. The Al plate was connected with the ground. Figure 2b depicts the calculated results of the electric potential distribution in the TENG under four different sliding distances of 0, 16, 26, and 40 mm. When two plates are fully overlapped, the electric

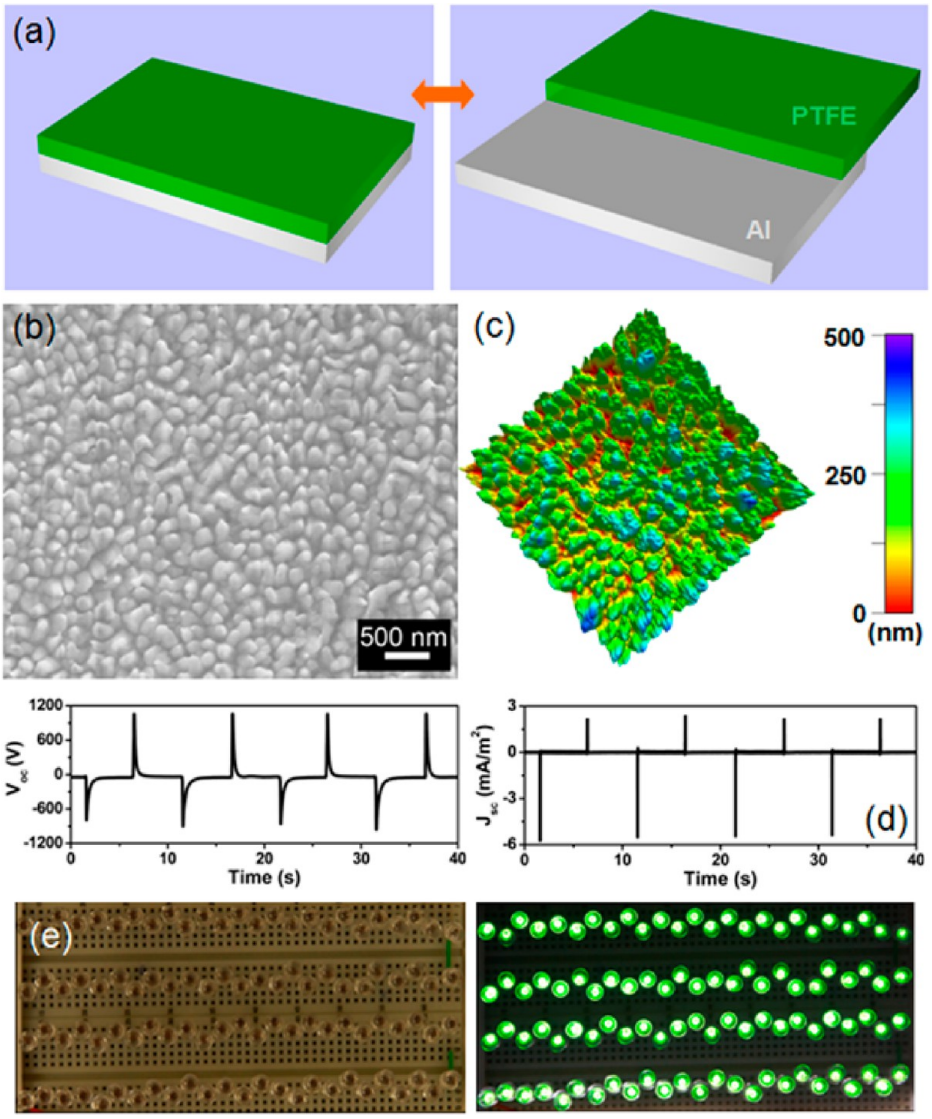

Figure 1. (a) Schematic diagram of the single-electrode-based sliding TENG. (b) SEM image of the PTFE surface with etched nanoparticle structure. (c) AFM image of the etched PTFE surface. (d) Open-circuit voltage (V_{oc}) and the short-circuit current density (J_{sc}) of the TENG. (e) Snapshot of 100 commercial green LEDs directly driven by the TENG with the fast sliding motion, as shown in the movie file 1.

potential on the PTFE surface approaches zero. When the top PTFE plate slides out with a displacement of 26 mm, the electric potential on the PTFE surface is up to −6000 V. It can be clearly seen that the electric potential difference between the PTFE and the Al increases dramatically with increasing sliding distance. As illustrated in Figure 2c, the amount of the total charges on the Al plate decreases linearly with increasing sliding distance, indicating that the transferred charges between Al and the ground increase with the increasing sliding distance.

Usually, the effective output power of the TENG depends on the match with the loading resistance. Figure 2d shows the resistance dependence of both output voltage and the output current density with the resistance from 10 Ω to 1 GΩ. The output voltage of the device rises up with increasing loading resistance, while the current density drops with the increase of the resistance. As shown in Figure 2e, the output power density was plotted as a function of the loading resistance. The instantaneous power density remains close to 0 with the resistance below 1 MΩ and then increases in the resistance region from 1 to 100 MΩ. The power density decreases under the larger loading resistance (>100 MΩ). The maximum value of the output power density reaches 350 mW/m^2 at a loading resistance of 100 MΩ.

To illustrate the potential applications of the single-electrode-based sliding TENG, we demonstrated that the TENG can be used as a self-powered sensor for detecting the sliding speed of an object. As shown in Figure 3a, the linear grating of the Al plate with a uniform period was fabricated, where the rows of grating units have the same size (5 mm × 40 mm)

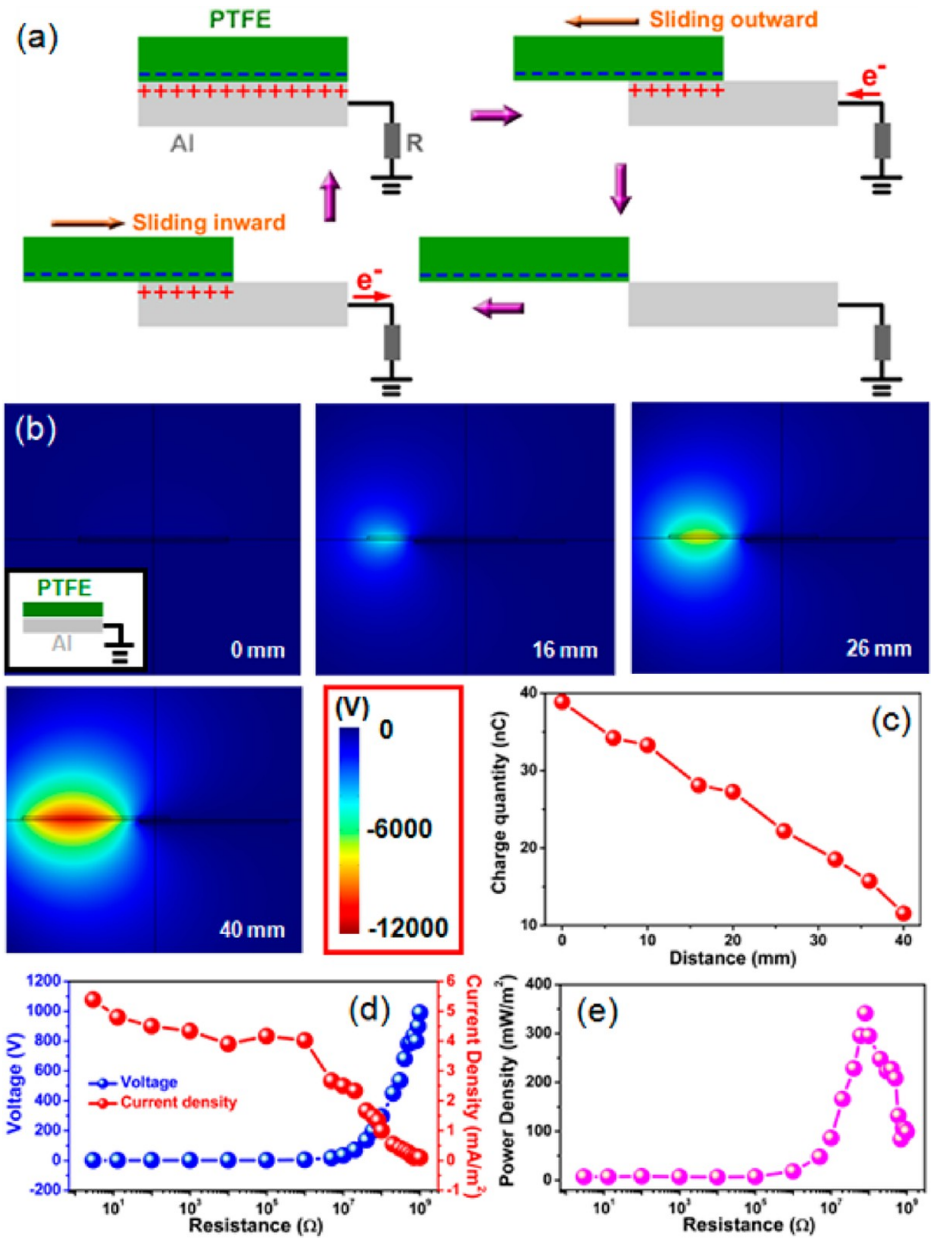

Figure 2. (a) Sketches that illustrate the electricity generation process in a full cycle. (b) Finite-element simulation of the potential distribution in the TENG. The inset shows the model for the calculation with the separation distance of 0.2 mm between PTFE and Al. (c) Curve of the induced charge quantity on the Al electrode *versus* the sliding distance from 0 to 40 mm. (d) Dependence of the output voltage and the current density on the external loading resistance. (e) Plot of the power density *versus* the loading resistance.

and all the Al strips are electrically connected together as an electrode across a loading resistor connected with the ground. A PTFE patch with a size of 2 cm × 2 cm was used as the sensitive unit, and a detected object was attached to it. When the PTFE slid through the Al strips, the output voltage of the TENG exhibits peaks of alternating directions, as illustrated in Figure 3a. The number of peaks with the negative direction correspond to the number of the Al strips. By fixing one end of the substrate and increasing the height of the other end (Figure S2), we measured the output voltages of the TENG under different tilt angles (defined as the angles between the substate and the ground), as shown in Figure 3b. Due to the increase of the gravity acceleration of the detected object, it slid faster and faster with increasing tilt angles, resulting in the decrease of the used time that the PTFE slid through the Al strips, as shown in Figure 3c. By using the output voltage peaks of the TENG, we can obtain the speed of the detected object plotted as a function of the sliding distance on the Al strips, as depicted in Figure 3d. The speed exhibits a linear increase with the sliding distance and can be up to 132 mm/s at the tilt angle of 10.5°. The speed can be increased further

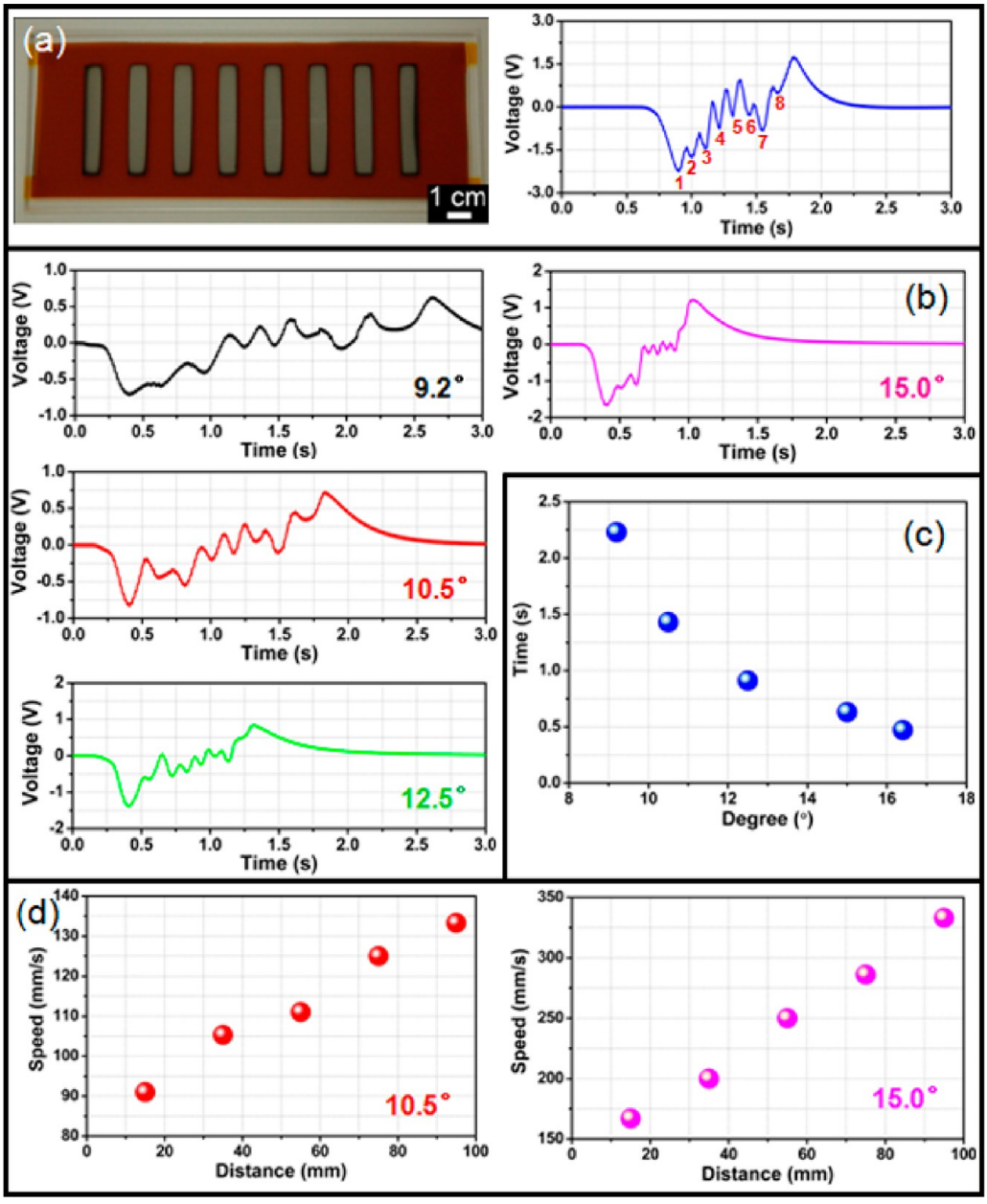

Figure 3. (a) Optical image of the fabricated Al electrode strips and the output voltage of the TENG when the PTFE slid through the Al electrodes. (b) Measured output voltages under the different tilt angles of the Al electrode plate, where the tilt angle was defined as the angle between the Al electrode plate and the ground. (c) Plot of the time from the first negative output voltage peak to the last positive one *versus* the different tilt angles of the Al electrode plate. (d) Summarized relationships between the speed and the distance under two different tilt angles.

to 330 mm/s by increasing the tilt angle of the Al plate to 15.0°.

To illustrate the potential applications of the single-electrode-based sliding TENG as the displacement vector sensor system, we fabricated 16 Al electrode channels distributed along four directions for detecting the movement direction and position of an object attached to the PTFE by real-time recording the output voltages in the 16 channels. Figure 4a shows the schematic diagram of the fabricated displacement vector sensor system, where each Al electrode is connected with an external loading resistance of 10 MΩ to the ground. The output voltage signals in 16 channels were recorded in real-time as a mapping figure. Figure 4b presents the photograph of the fabricated sensor system, where each Al electrode strip has a size of 5 mm × 30 mm. The detected object was attached to a PTFE patch with the size of 2 cm × 2 cm, which was used as the sensitive unit at the center of the sensor system. To demonstrate the functionality of the fabricated sensor system, the PTFE slid along the direction 1 to contact the first Al electrode strip, and the corresponding output voltages in the 16 channels were measured in real-time, as shown in Figure 4c.

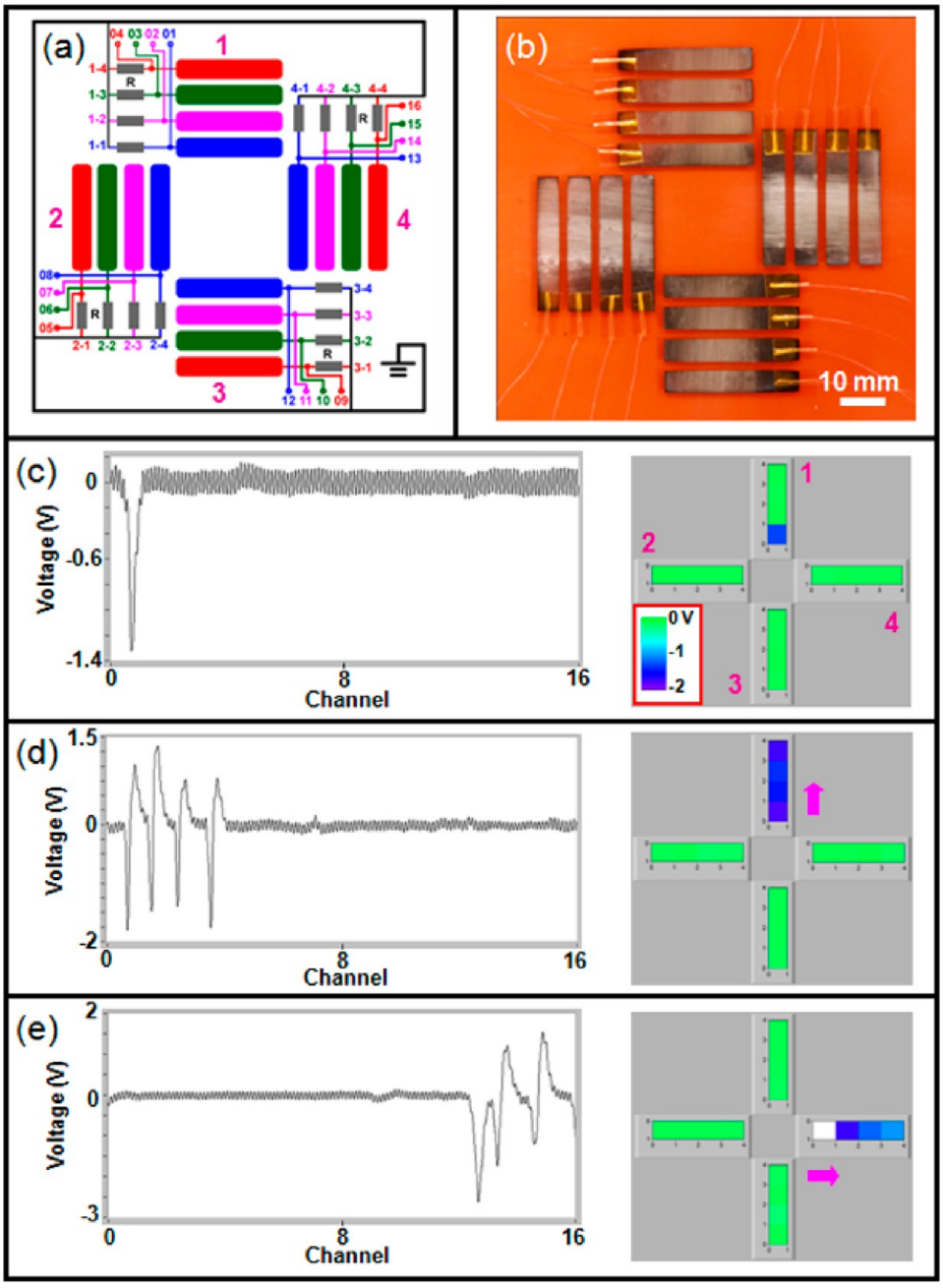

Figure 4. (a) Schematic diagram of the fabricated displacement vector sensor system. (b) Optical image of the sensor system. (c) Output voltages in 16 channels and the obtained mapping figure when the PTFE was in contact with the first Al strip. (d) Output voltages in 16 channels and the mapping figure when the PTFE slid rapidly along the direction 1. (e) Output voltages in 16 channels and the mapping figure when the PTFE slid rapidly along the direction 4.

A negative output voltage peak of about −1.3 V can be observed in the first channel, which corresponds to the contact between the PTFE and the first Al electrode strip. The mapping figure of the measured negative output voltage signals also shows that the first Al electrode strip was touched by the PTFE. Without the displacement of the PTFE, the corresponding mapping figure shows that no output voltage signals can be observed, as illustrated in Figure S3. If a smaller loading force on the PTFE was applied, the TENG produced a lower output voltage of −0.7 V due to the decrease of the induced triboelectric charges, as shown in Figure S4.

When the detected object slid rapidly through the Al electrode strips along the direction 1, the measured output voltage signals in 16 channels were depicted in Figure 4d, clearly showing that the four negative output voltages of about −1.8 V can be observed in the first 4 channels along the direction 1. Analysis of the corresponding mapping figure can also reveal that the detected object slid along the direction 1. Figure 4e shows the output voltage signals in the 16 channels

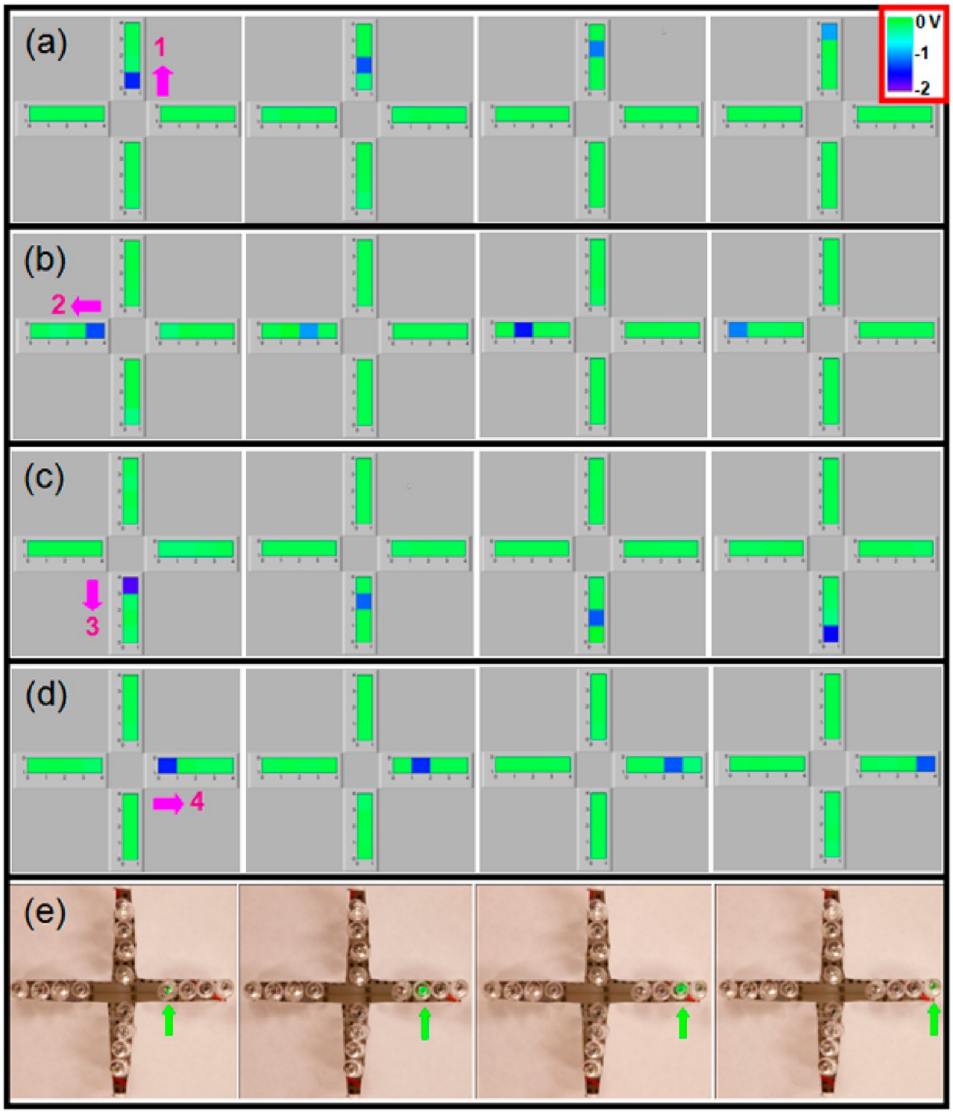

Figure 5. (a–d) Produced mapping figures when the PTFE slid through the Al strips along the different four directions. (e) Green LEDs were lighted up one by one when the PTFE slid along the direction 4.

and the mapping figure when the detected object slid rapidly along the direction 4. The obtained negative output voltage signals decrease in the Al electrode channels from inside to outside, which is associated with the decrease of the loading force on the PTFE in the sliding process. Figures S5 and S6 show the obtained mapping figures of the sensor system when the PTFE slid rapidly along the other two directions. These results clearly indicate that all of the 16 channels of the device are functional and the sensor system can be used to determine the sliding direction of the detected object under the fast movement. Moreover, the fabricated sensor system has a fast response to the displacement of the detected object since it can produce a negative output voltage signal immediately when the PTFE is just in contact with the Al electrode strip.

By addressing and monitoring the negative output voltage signals in 16 channels of the vector sensor system, the displacement information of the detected object including the direction and position can be attained. As displayed in Figure 5a, the measured four mapping figures of the sensor system clearly show the four different positions when the detected object slid through the direction 1. The difference between the mapping figures in Figure 5a,d is due to the different sliding speeds. As shown in Figure 5a, when the PTFE was in contact with the first Al electrode strip, a negative output voltage signal was produced in the first channel. Then, when the sliding PTFE was in contact with the second Al electrode strip, a negative output voltage signal can be obtained in the second channel, but there was no negative output voltage signal in the first channel due to no change of the contact area between the PTFE and the first Al electrode strip, as shown in Figure 5a. However, when the sliding speed of the PTFE was enough fast, the produced negative output voltage signals in the several channels can be observed in the same mapping figure,

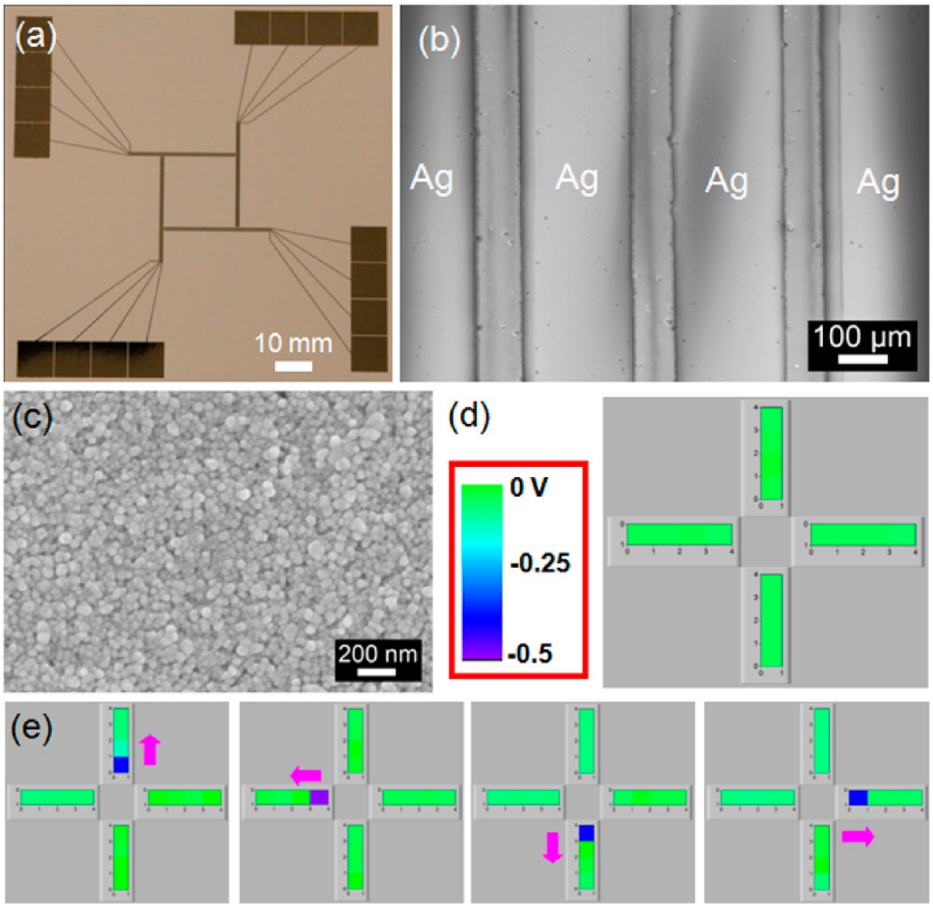

Figure 6. (a) Photograph of the fabricated displacement vector sensor system by using Ag electrodes. (b) SEM image of the Ag electrodes. (c) SEM image of the enlarged Ag electrode. (d) Mapping figure when the PTFE did not slide, showing that no output voltage signals can be observed. (e) Measured mapping figures when the PTFE slid to contact the first Ag electrode along the four different directions.

as shown in Figure 4d. Figure 5b–d shows the obtained mapping figures of the sensor system when the detected object slid along the other three directions. The motion direction and position of the detected object can be confirmed by the analysis of the mapping figure. Figure S7 presents the positive output voltage signals that can also be used to detect the direction and position, which has been shown in movie file 2 (see the Supporting Information). However, the resolution of displacement for this case is substantially lower than that of negative output voltage signals since the positive output voltage signals can only be produced when the PTFE patch fully slides out of the contacted Al strip, thus the displacement detection limit is larger than the size of the used PTFE plate. However, the resolution of the displacement for the negative output voltage signals is determined by the width of the fabricated Al strips.

To demonstrate that the induced mechanical energy by the sliding motion of the detected object in the sensor system can be used to detect the sliding direction and position, 16 green LEDs were used to replace the loading resistors in Figure 4a as the displacement indicators. When the detected object slid along the direction 4, the produced energy at the different positions can drive the different LEDs, so that the corresponding LEDs can be lighted up one by one, as illustrated in Figure 5e. The other LEDs can be also lighted up when the detected object slid along the other directions, as shown in the movie file 3 (see the Supporting Information). The direction and position of the detected object can be confirmed by observing which LED in the sensor system is emitting light. The results are consistent with the data in Figure 5a–d.

In order to enhance the detection resolution of the displacement vector sensor, the inkjet-printed Ag microstrips on the paper substrate were designed to fabricate the device. Figure 6a shows the photograph of the printed Ag microstrips, where the width of each Ag strip is about 150 μm with the separation distance of 50 μm, as illustrated in Figure 6b. The enlarged SEM image of the Ag electrode strip clearly shows that the diameters of the Ag nanoparticles are smaller than 50 nm, as shown in Figure 6c. When the detected object remains at the center of the system, the mapping figure of the negative output voltage signals shows that no output signals for all 16 channels can be observed, as shown in Figure 6d. Figure 6e displays

the measured mapping figures of the sensor system when the detected object on the PTFE slightly slid to contact the first Al electrode microstrip along the four directions. Although the measured output voltages are smaller than the data in Figure 4 due to the smaller electrode size, the obtained displacement resolution of about 200 μm is much higher than that in Figure 4. Moreover, when the PTFE slid rapidly through the Al microstrips along the direction 4, the negative output voltage signals in the four channels can be observed, as shown in Figure S8.

CONCLUSION

In summary, we have demonstrated a designed TENG based on the sliding motion between a PTFE patch and an Al plate without need of the metal deposition on the triboelectric materials. The mechanism of the TENG is based on the charge transfer between the Al electrode and the ground by modulating the relatively sliding distance between the Al and PTFE, thus generating an AC electric output across an external load. By converting the mechanical energy of sliding motion into electricity, the TENG delivered an open-circuit voltage of 1100 V and a short-circuit current density of about 6 mA/m^2, which can be directly used to drive 100 green LEDs. The TENG based on the linear grating of the Al electrode can be used as a self-powered displacement sensor for detecting the speed along one direction. Moreover, the fabricated 16 Al electrode channels were distributed along four different directions, which was used as a displacement vector sensor system for detecting the direction and position of an object at the center. The displacement information can be obtained by analysis of the real-time recording negative output voltage signals in the 16 channels as a mapping figure. This work opens up a new field in single-electrode-based sliding nanogenerators for harvesting mechanical energy and pushes forward a significant step toward the practical applications of nanogenerators as the self-powered sensor systems.

EXPERIMENTAL SECTION

Fabrication of the Single-Electrode-Based Sliding TENG and the Self-Powered Displacement Vector Sensor System. The fabricated TENG is based on the sliding motion between a PTFE patch with the etched nanoparticles on the surface and an Al electrode, which was connected to the ground across an external loading resistor. The nanoparticle structures with the average diameter of about 200 nm on the PTFE surface were fabricated by using the inductively coupled plasma (ICP) reactive ion etching. In the etching process, a Au film with the thickness of about 30 nm as the mask was deposited on the PTFE surface. A mixed gas including Ar, O_2, and CF_4 was introduced in the ICP chamber, where the corresponding flow rates are 15.0, 10.0, and 30 sccm, respectively. The PTFE nanoparticle structure was etched under one power source of 400 W to generate a large density of plasma. For the self-powered displacement vector sensor system, an acrylic mask was fabricated by using the laser cutting technique. Then Al was deposited through the open window areas of the mask to produce the strip structure. The 16 Al electrode strips were distributed along four different directions, and each Al electrode was connected with a loading resistor of 10 MΩ. The other end of the loading resistor was connected with the ground. A PTFE patch was placed at the center of the sensor system as the sensitive unit, where the detected object was attached to the PTFE.

Measurement of the Fabricated Self-Powered Displacement Vector Sensor System. In the voltage measurement process, the displacement vector sensor system was connected with both a low-noise voltage preamplifier (Stanford Research System model SR560) and a loading resistor of about 10 MΩ, where the other end of the resistor was connected with the ground. A homemade data acquisition system was used to obtain the output voltage signals of the 16 channels in real-time. For the current measurement, the output current of the TENG was measured by a low-noise current preamplifier (Stanford Research SR570). The output voltage of the TENG was measured by an electrometer with very large input resistance.

Conflict of Interest: The authors declare no competing financial interest.

Acknowledgment. This work was supported by U.S. Department of Energy, Office of Basic Energy Sciences (DE-FG02-07ER46394), NSF, and the Knowledge Innovation Program of the Chinese Academy of Sciences (KJCX2-YW-M13). The authors thank Taoran Le for the help of the electrode fabrication.

Supporting Information Available: Additional figures include the schematic diagram of the connection between the green LEDs and the TENG, the schematic diagram of the sliding process of the PTFE on a tilted substrate with the periodic Al strips, the mapping figure without the sliding motion of the PTFE, the mapping figure when the PTFE slid to contact the first Al strip under a smaller loading force along the direction 1 in Figure 4c, the mapping figure when the PTFE slid rapidly along the direction 2, the mapping figure when the PTFE slid rapidly along the direction 3, the mapping figures when the positive output voltage signals were used to detect the displacement, and the mapping figure when the PTFE slid rapidly along the direction 4 for the device in Figure 6. The additional movie files include single-electrode-based sliding TENG for directly lighting up 100 LEDs, the output voltage signals when the PTFE slid rapidly along the different directions, and the LEDs lighted up by the sliding motion of PTFE along the different directions. This material is available free of charge *via* the Internet at http://pubs.acs.org.

REFERENCES AND NOTES

1. Wang, Z. L.; Zhu, G.; Yang, Y.; Wang, S.; Pan, C. Progress in Nanogenerators for Portable Electronics. *Mater. Today* **2012**, *15*, 532–543.
2. Guang, Z.; Pan, C.; Guo, W.; Chen, C.-Y.; Zhou, Y.; Yu, R.; Wang, Z. L. Tiboelectric-Generator-Driven Pulse Electrodeposition for Micropatterning. *Nano Lett.* **2012**, *12*, 4960–4965.
3. Yang, Y.; Zhang, H.; Lee, S.; Kim, D.; Hwang, W.; Wang, Z. L. Hybrid Energy Cell for Degradation of Methyl Orange by Self-Powered Electrocatalytic Oxidation. *Nano Lett.* **2013**, *13*, 803–808.
4. Rome, L. C.; Flynn, L.; Goldman, E. M.; Yoo, T. D. Generating Electricity While Walking with Loads. *Science* **2005**, *309*, 1725–1728.
5. Williams, C. B.; Shearwood, C.; Harradine, M. A.; Mellor, P. H.; Birch, T. S.; Yates, R. B. Development of an Electromagnetic Micro-Generator. *IEE Proc., Circuits Devices Syst.* **2001**, *6*, 337.
6. Nguyen, T. D.; Deshmukh, N.; Nagarah, J. M.; Kramer, T.; Purohit, P. K.; Berry, M. J.; McAlpine, M. C. Piezoelectric Nanoribbons for Monitoring Cellular Deformations. *Nat. Nanotechnol.* **2012**, *7*, 587–593.
7. Chang, C.; Tran, V. H.; Wang, J.; Fuh, Y.-K.; Lin, L. Direct-Write Piezoelectric Polymeric Nanogenerator with High Energy Conversion Efficiency. *Nano Lett.* **2010**, *10*, 726–731.

8. Herb, R. G.; Parkinson, D. B.; Kerst, D. W. The Development and Performance of an Electrostatic Generator Operating under High Air Pressure. *Phys. Rev.* **1937**, *51*, 75–83.
9. Mitcheson, P. D.; Miao, P.; Stark, B. H.; Yeatman, E. M.; Holmes, A. S.; Green, T. C. MEMS Electrostatic Micropower Generator for Low Frequency Operation. *Sens. Actuators, A* **2004**, *115*, 523–529.
10. Fan, F.-R.; Tian, Z.-Q.; Wang, Z. L. Flexible Triboelectric Generator. *Nano Energy* **2012**, *1*, 328–334.
11. Wang, S.; Long, L.; Wang, Z. L. Nanoscale Triboelectric-Effect-Enabled Energy Conversion for Sustainably Powering Portable Electronics. *Nano Lett.* **2012**, *12*, 6339–6346.
12. Lin, L.; Wang, S.; Xie, Y.; Jing, Q.; Niu, S.; Hu, Y.; Wang, Z. L. Segmentally Structured Disk Triboelectric Nanogenerator for Harvesting Rotational Mechanical Energy. *Nano Lett.* **2013**, *13*, 2916–2923.
13. Wang, Z. L.; Wu, W. Nanotechnology-Enabled Energy Harvesting for Self-Powered Micro/Nanosystems. *Angew. Chem., Int. Ed.* **2012**, *51*, 11700–11721.
14. Yang, Y.; Zhou, Y.; Wu, J. M.; Wang, Z. L. Single Micro/Nanowire Pyroelectric Nanogenerators as Self-Powered Temperature Sensors. *ACS Nano* **2012**, *6*, 8456–8461.
15. Lin, Z. H.; Zhu, G.; Zhou, Y. S.; Yang, Y.; Bai, P.; Chen, J.; Wang, Z. L. A Self-Powered Triboelectric Nanosensor for Mercury Ion Detection. *Angew. Chem., Int. Ed.* **2013**, *125*, 5169–5173.
16. Lin, Z. H.; Xie, Y.; Yang, Y.; Wang, S.; Zhu, G.; Wang, Z. L. Enhanced Triboelectric Nanogenerators and Triboelectric Nanosensor Using Chemically Modified TiO_2 Nanomaterials. *ACS Nano* **2013**, *7*, 4554–4560.
17. Yang, Y.; Lin, L.; Zhang, Y.; Jing, Q.; Hou, T.-C.; Wang, Z. L. Self-Powered Magnetic Sensor Based on a Triboelectric Nanogenerator. *ACS Nano* **2012**, *6*, 10378–10383.
18. Wilson, J. S. *Sensor Technology Handbook*; Newnes: Oxford, U.K., 2005; ISBN: 0-7506-7729-5.
19. Ng, T. W. The Optical Mouse as a Two-Dimensional Displacement Sensor. *Sens. Actuators, A* **2003**, *107*, 21–25.
20. Yaralioglu, G. G.; Atalar, A.; Manalis, S. R.; Quate, C. F. Analysis and Design of an Interdigital Cantilever as a Displacement Sensor. *J. Appl. Phys.* **1998**, *83*, 7405–7415.
21. Lantz, M. A.; Binnig, G. K.; Despont, M.; Drechsler, U. A Micromechanical Thermal Displacement Sensor with Nanometre Resolution. *Nanotechnology* **2005**, *16*, 1089–1094.
22. Miller, M. M.; Prinz, G. A.; Lubitz, P.; Hoines, L.; Krebs, J. J.; Cheng, S. F.; Parsons, F. G. Novel Absolute Linear Displacement Sensor Utilizing Giant Magnetoresistance Elements. *J. Appl. Phys.* **1997**, *81*, 4284–4286.
23. Cross, J. A. *Electrostatics: Principles, Problems and Applications*; Adam Hilger: Bristol, U.K., 1987; Chapter 2.
24. Saurenbach, F.; Wollmann, D.; Terris, B. D.; Diaz, A. F. Force Microscopy of Ion-Containing Polymer Surfaces: Morphology and Charge Structure. *Langmuir* **1992**, *8*, 1199–1203.